

Reduction of dislocation density and dislocation analysis of MOVPE grown GaN layers

Frank Habel¹⁾, Matthias Seyboth¹⁾

1) Optoelectronics Department, University of Ulm, 89069 Ulm, Germany

Due to the rapid progress in the development of high-end GaN based devices such as laser diodes, ultra violet light emitting diodes and field effect transistors the role of threading dislocations is getting more and more important. The dislocation density in common heteroepitaxially grown GaN on sapphire or silicon carbide substrates is in the order of $10^8 - 10^{10} \text{cm}^{-2}$, due to the lattice mismatch between these substrates and GaN together with the resulting columnar structure of the grown layers.

Dislocations have several strong effects on devices. Especially for laser diodes, a low dislocation density is a prerequisite for long device lifetimes. Moreover, dislocations act as non-radiative recombination centers [1], reducing the efficiency of optoelectronic devices especially in the violet and UV range [2]. Carrier mobility is affected by scattering at charged dislocation lines. The formation of V-defects during growth of InGaN quantum wells is correlated with dislocations [3].

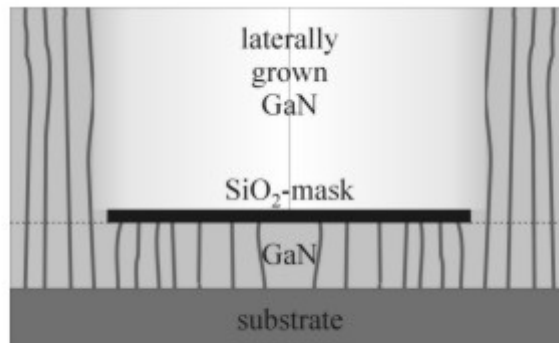


Fig. 1: ELOG schematic

One of the most promising techniques to reduce the dislocation density is the growth on structured substrates. The basic method is epitaxial lateral overgrowth (ELOG) [4], which benefits from the fact, that dislocations usually run vertically from the substrate interface right to the surface of the semiconductor layer, whereas laterally grown crystal areas are nearly dislocation free (Fig. 1). An advanced method is the facet assisted epitaxial lateral overgrowth (FACELO) [5], where the propagation of the dislocations is affected by appropriate control of the dominating crystal facets during growth. Even in the commencing mass production of low-dislocation GaN substrates an understanding of the influence of growth parameters on the crystal facets is very important, e.g. as Sumitomo Electric Industries' dislocation elimination by epitaxial growth with inverse-pyramidal pits (DEEP) technique for production is also based on the bending of dislocations at crystal facets during growth [6].

To investigate these relations we performed epitaxial growth on structured substrates in an Aixtron 200/4 RFS horizontal reactor system. The growth temperature was varied between 1020°C and 1130°C at reactor pressures between 100 and 400mbar. The V-III ratio was kept at 950. As templates 1µm thick GaN layers on sapphire substrate were used. The mask material was 250nm SiO₂ deposited by PECVD. A pattern consisting of stripes with various widths and distances was chosen to study the influence of the mask geometry. The stripe arrays were orientated along the $\langle 1-100 \rangle$ or the $\langle 11-20 \rangle$ directions, respectively. Etching of the mask was performed in a CF₄ RIE system.

In order to minimize the dislocation density and to optimize the coalescence of the layers, we studied the influence of the major process parameters on the lateral and vertical growth rate and the cross sectional shape of the crystals grown on ELOG stripe masks. For these experiments the anisotropic growth of GaN has to be taken into account.

In Fig. 2a–c the influence of the process temperature on the lateral and vertical growth rates as well as the cross sectional shape can be seen for ELOG stripes in $\langle 1-100 \rangle$ direction. For low temperatures a triangular shape with sidewalls formed by $\{11-22\}$ facets predominates. With increasing process temperature the shape shifts via a combination of trapezoidal and rectangular to rectangular, confined by $\{11-20\}$ facet sidewalls, due to an increasing lateral growth rate. A reduced reactor pressure also leads to an increase in lateral growth. On the other hand no effect of these parameters can be seen for ELOG stripes in $\langle 11-20 \rangle$ direction, where a triangular cross section was found for all studied sets of parameters because of a strong domination of $\{1-101\}$ facets as sidewalls (Fig. 2d).

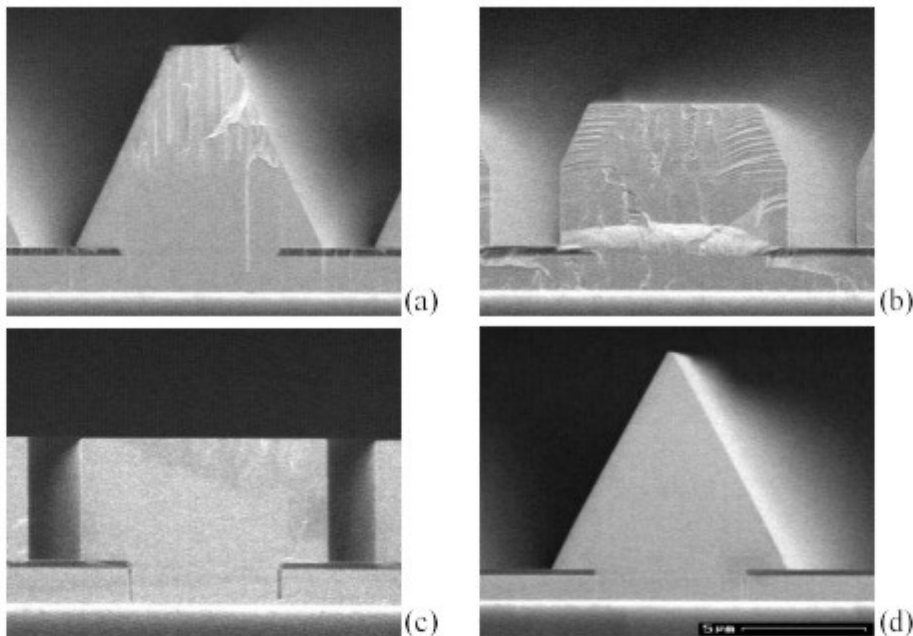


Fig. 2: Varying cross section for growth on stripes in $\langle 1-100 \rangle$ direction and growth temperature of 1020°C (a), 1070°C (b) and 1130°C (c). Low temperatures lead to a triangular and high temperatures to a rectangular cross section. For stripes in $\langle 11-20 \rangle$ direction the cross section remains unchanged (d).

Another important point is the dependence of the growth rate on the surrounding masked area, i.e. in the case of stripe masks on the width of the SiO_2 stripes. To study this effect, our ELOG mask has an array of SiO_2 stripes varying in width from 20 μm to 300 μm separated by 8 μm wide mask openings. Within this array the height of the grown structures changed from 5.2 μm for small distances of the mask openings to 22.2 μm for large distances. For better understanding of this effect, the deposited crystal volumes per wafer area are plotted versus the width of the stripes in Fig. 3. Except for the array borders, where growth is possibly affected by the surrounding mask structure, this value shows only a slight change. So for mask design it has to be taken into consideration that in first approximation the deposited material per wafer area can be regarded as constant. However, a dependence of the cross sectional shape on the distance of the mask openings was observed. While rectangular cross sections with $\{11-20\}$ facet sidewalls were found for small stripes, a combination of rectangular and trapezoidal cross section (similar to Fig. 2b) was found on the same sample for wide stripes. Thus the dominance of certain crystal facets cannot be explained by the general growth parameters, but by a change of local process conditions on the surface.

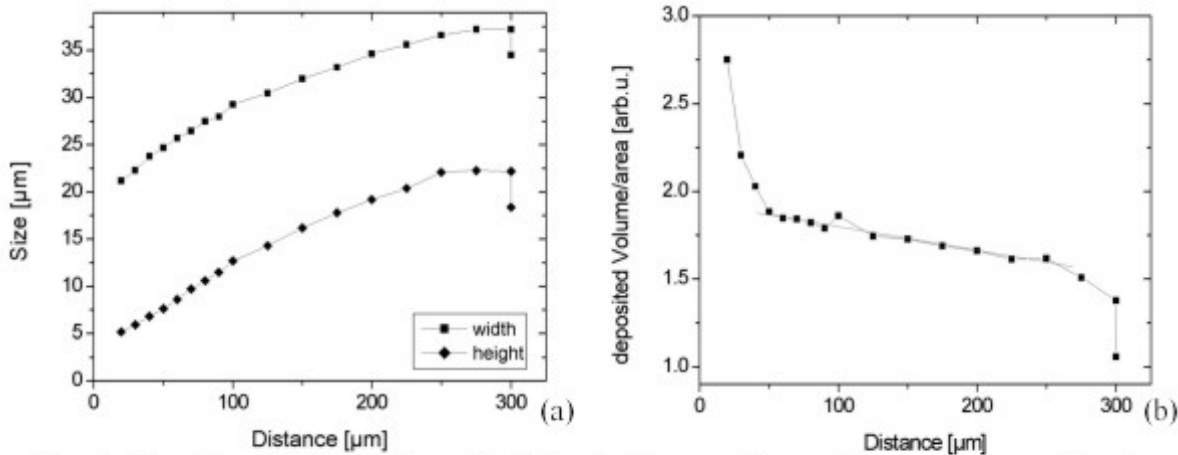


Fig. 3: Growth on ELOG masks with different distances between the growth areas. The size of the grown structures increases with distance (a). The deposited Volume per wafer area remains almost constant (b).

Based on these experiments we grew completely coalesced 2 inch ELOG wafers. For these structures a stripe width of 8μm and 3μm mask openings were used. The thickness of the ELOG–layer is 4.3μm. In Fig. 4a a XRD–scan of this structure is plotted. As the dotted curves indicate, the plot consists of two signals originating from the wings and a smaller signal from the post region. The tilt angle between the post and wing regions is 0.15°. Fig. 4b shows an AFM surface profile of the same sample. Here a wing tilt of 0.17° was found confirming the x–ray results.

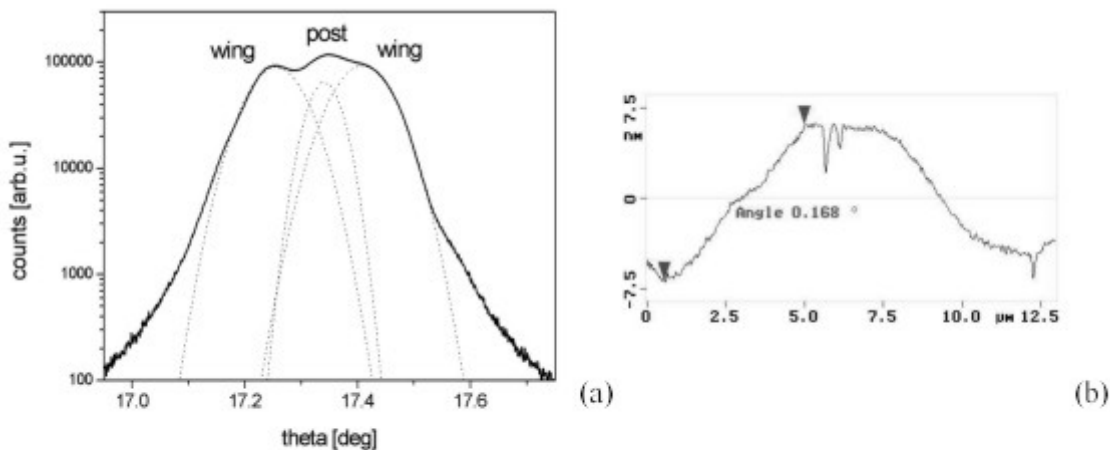


Fig. 4: The wing tilt of the ELOG structures was determined by XRD-scans (a) and by AFM (b). The measured values are 0.15° and 0.17°, respectively.

In order to measure the dislocation density, we investigated the hydrogen chloride vapor phase etching technique, which was first demonstrated by Sony [7]. The sample is exposed to HCl diluted by nitrogen at elevated temperatures. The details for this process can be found in [8]. Etching occurs predominantly where the crystal structure is disturbed by dislocations penetrating the surface, and pits are formed which make the dislocations visible. The etch pits can be observed by scanning electron microscopy as well as by atomic force microscopy. Figure 5 depicts an AFM scan of an etched ELOG sample. For the vertically grown post region an etch pit density of $3.5 \times 10^8 \text{cm}^{-2}$ was determined, whereas the dislocation density in the laterally grown wing regions is below $1.2 \times 10^7 \text{cm}^{-2}$. In the coalescence region a line of etch pits is visible.

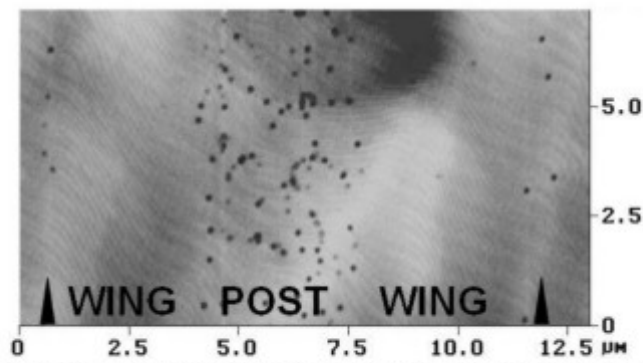


Fig. 5: Distribution of dislocations on a coalesced ELOG sample. Coalescence lines are indicated by arrows

To further reduce the dislocation density, FACELO structures were realized. In the first step a low growth temperature and a higher reactor pressure were used to form triangular cross sections with $\{11\bar{2}2\}$ facets. Then a coalesced layer was grown in the next step under higher temperature and low reactor pressure. In Fig. 6 AFM scans of an etched sample are shown. The width of the mask openings is $4\mu\text{m}$ (Fig. 6a), $6\mu\text{m}$ (Fig. 6b) and $8\mu\text{m}$ (Fig. 6c). For $4\mu\text{m}$ mask openings no post region with higher dislocation density at the surface can be found. For the larger structures the width of the high dislocation density area is $1.5\mu\text{m}$ and $3.5\mu\text{m}$, respectively. Thus the FACELO technique allowed a reduction of the width of this area by $4.5\mu\text{m}$. Using smaller mask openings, the growth of low dislocation material over large areas is possible.

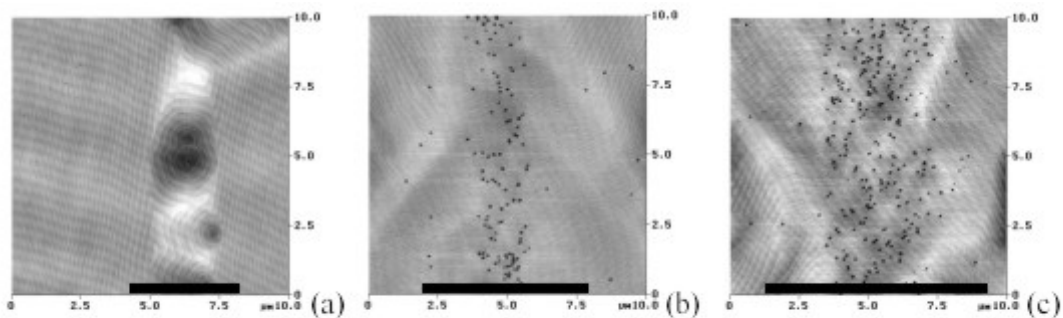


Fig. 6: Dislocation distribution on FACELO structures: mask openings of $4\mu\text{m}$ (a), $6\mu\text{m}$ (b) and $8\mu\text{m}$ (c). The width of the high dislocation area is reduced by about $4.5\mu\text{m}$

Acknowledgement:

We gratefully acknowledge fruitful discussions with F. Scholz. This research was supported by the Bundesministerium für Bildung und Forschung (BMBF) Germany under contract No. 01BS-1-51.

- [1] D. Cherns, S.J. Henley and F.A. Ponce, *Appl. Phys. Lett.* 78, 2691 (2001)
- [2] T. Stephan, M. Kunzer, P. Schlotter, W. Pletschen, H. Obloh, S. Müller, K. Köhler, and J. Wagner, *phys. stat. sol. (a)* 194, 568 (2002).
- [3] J.S. Speck, S.J. Rosner, *Physica B* 273–274, 24 (1999)
- [4] B. Beaumont, P. Vennéguès and P. Gibart, *phys. stat. sol. (b)* 227, 1 (2001)
- [5] H. Miyake, R. Takeuchi, K. Hiramatsu, H. Naoi, Y. Iyechika, T. Maeda, T. Riemann, F. Bertram and J. Christen, *phys. stat. sol. (a)* 194, 545 (2002)
- [6] Sumitomo Electric Industries, Ltd., http://www.sei.co.jp/sn/2002/07/feature_article.html (2002)
- [7] T. Hino, S. Tomiya, T. Miyajima, K. Yanashima, S. Hashimoto and M. Ikeda, *Appl. Phys. Lett.* 76, 3421 (2000)
- [8] F. Habel, M. Seyboth, to be published in *phys. stat. sol. (c)*